Journal of Cleaner Production 242 (2020) 118421

Contents lists available at ScienceDirect

Journal of Cleaner Production

journal homepage: www.elsevier.com/locate/jclepro

A cleaner and more sustainable decarbonation process via ionic-liquid absorption for natural gas with high carbon dioxide content

Lara Costa Barbosa, Marina Vilhena da C. Nascimento, Ofélia de Queiroz F. Araújo, José Luiz de Medeiros*

Escola de Química, Federal University of Rio de Janeiro, Av. Horacio Macedo, 2030, Bl. E, 21949-900, Rio de Janeiro, RJ, Brazil

ARTICLE INFO

Article history:
Received 1 March 2019
Received in revised form
11 August 2019
Accepted 13 September 2019
Available online 18 September 2019

Handling Editor: Prof. Jiri Jaromir Klemeš

Keywords:
CO_2 capture
Ionic-liquid
Solvent screening
Multi-criterial analysis
Sustainability analysis

ABSTRACT

Ionic-liquids are considered alternatives to conventional aqueous-amines absorption solvents due to their carbon dioxide affinity, low vapor-pressure, high thermal stability and low heat-ratio. In this context, this work firstly approaches a new natural gas decarbonation process based on ionic-liquid [Bmim][NTf_2] absorption and selective solute stripping at high-pressure and high-temperature (2-staged-stripping initiating at 50 bar and 250 °C) taking advantage of the high thermal resistance of halogenated ionic-liquids. Its strong points have to do with its high-pressure stripping (50 bar) which impressively lowers carbon dioxide compression power for enhanced oil recovery destinations. Consequently, such new process burns less fuel for power production and is a cleaner production alternative to traditional aqueous-amine-based decarbonation processes which strip carbon dioxide at only 1–2 bar. Secondly, the positive aspects of new ionic-liquid decarbonation process were confirmed in two new multi-criterial sustainability-related implemented procedures: (i) new ionic-liquid multi-criterial screening for natural gas decarbonation; and (ii) new multi-criterial sustainability assessment of natural gas decarbonation processes. The new multi-criterial screening confirmed the same [Bmim][NTf_2] as the most suited ionic-liquid from environment/engineering relevant properties (e.g., carbon dioxide loading, absorption-related properties, toxicology and cost), while the multi-criterial sustainability assessment proved that the new [Bmim][NTf_2] decarbonation process is five times cleaner and more sustainable than the amine-based counterpart, both respectively attaining sustainability degrees of *5.17* and *1.0*. In this sustainability assessment, the two decarbonation processes were designed for cleaning natural gas with 45%mol carbon dioxide at 60 bar. Processes were scored in terms of compliance to qualitative heuristic criteria and quantitative sustainability metrics for environmental-economic-social aspects. Metrics were aggregated into one indicator, the sustainability degree, evoking a sustainability-based process ranking.

1. Introduction

The necessity of low-carbon energy sources makes carbon capture, storage and utilization important to meet CO_2 emissions reduction targets (Leung et al., 2014). In this context, fossil-fuels with a lower carbon footprint per power unit become more attractive than high emitting ones (e.g., coal). This is the case of natural gas (NG) with worldwide growing utilization. With raw water-saturated CO_2-rich NG, some conditioning is necessary: (i) dehydration for water dew-point adjustment (WDPA); (ii) propane and heavier hydrocarbons (C_3^+) removal for hydrocarbon dew-point adjustment (HCDPA); and (iii) CO_2 removal, where compressed CO_2 can be geologically stored or traded as enhanced oil recovery (EOR) agent (Arinelli et al., 2017).

Typical decarbonation technologies of CO_2-rich NG include absorption (de Medeiros et al., 2013), membrane-permeation (Arinelli et al., 2017) and cryogenic-distillation (Holmes and Ryan, 1982). Among them, aqueous-alkanolamine chemical-absorption – e.g.,

Abbreviations: C3+, Propane and Heavier Alkanes; CW, Cooling-Water; EOR, Enhanced Oil Recovery; HCDPA, Hydrocarbon Dew-Point Adjustment; IL, Ionic-Liquid; MEA, Monoethanolamine; MDEA, Methyl-diethanolamine; MMSm3/d, Millions of Standard m3/d; NG, Natural Gas; PHW, Pressurized-Hot-Water; PR-EOS, Peng-Robinson Equation-of-State; RK-EOS, Redlich-Kwong Equation-of-State; THF, Thermal-Fluid; VLE, Vapor-Liquid Equilibrium; WDPA, Water Dew-Point Adjustment.

* Corresponding author.
E-mail addresses: laracb@eq.ufrj.br (L.C. Barbosa), marinavcn@eq.ufrj.br (M.V.C. Nascimento), ofelia@eq.ufrj.br (O.Q.F. Araújo), jlm@eq.ufrj.br (J.L. de Medeiros).

https://doi.org/10.1016/j.jclepro.2019.118421
0959-6526/

methyl-diethanolamine (MDEA) and monoethanolamine (MEA) – is the most mature alternative. Despite its high CO_2/CH_4 selectivity, aqueous-amine chemical-absorption entails environmental-economic penalties such as solvent losses, high regeneration heat-ratio, degradation and corrosion (Huang et al., 2014).

Ionic-liquids (ILs) have been proposed as green solvents for NG decarbonation due to high thermal stability, good CO_2 solubility, low vapor-pressure and low regeneration heat-ratio (Valencia-Marquez et al., 2017). IL cation-anion combinations allow synthesizing ILs with tailor-made properties for specific applications (Vega et al., 2010). Despite their comparative advantages to aqueous-amines, ILs also have comparative issues: higher prices and viscosities. At laboratory-scale IL costs attain ≈1000USD/kg, potentially falling to ≈40US/kg at large-scales, still ≈80 times higher than aqueous-amines (Ramdin et al., 2012). Alternatives to overcome this penalty prescribe IL blends with amines and/or water. Since drying represents a non-negligible IL production cost, IL-water blends become attractive, additionally reducing solvent viscosity (Zeng et al., 2017). CO_2 solubility in aqueous [Bmim][NO_3] was found to be slightly higher than in pure IL for low water contents, gradually decreasing for high water contents (Bermejo et al., 2008).

Many works evaluated ILs for gas decarbonation. Shiflett et al. (2010) designed a flue-gas decarbonation with [Bmim][Ac] for coal-fired power plants decreasing 16% of heat-ratio and 11% of investment relatively to aqueous-MEA. Liu et al. (2016) assessed shale-gas decarbonation using [Bmim][NTf_2] with multi-stage solvent regeneration reducing 66.04% of heat-ratio (kJ/kgCO_2) relative to aqueous-MEA. Ma et al. (2018) studied [Bmim][NTf_2] for flue-gas decarbonation attaining 30.01% heat-ratio savings and 29.99% cost savings comparatively to aqueous-MEA absorption. Zubeir et al. (2018) modeled in ASPEN-PLUS a process with physical-sorbent IL [C6mim][TCM] for decarbonation of synthetic NG (46%mol CO_2) absorbing CO_2 at $P = 28$ bar, where the most interesting variant strips CO_2 at $P = 28$ bar and high-temperature ($T = 336^oC$) achieving great savings of CO_2 compression power to EOR. Zareiekordshouli et al. (2018) experimentally studied flue-gas (8%mol CO_2) decarbonation with chemical-sorbent IL [Emim][Ac] for $P(bar) \in [5,8]$ and $T(^oC) \in [25,65]$, removing 90% of CO_2 with lower stripping heat-ratio ($2.75GJ/t_{CO2}$) than aqueous-MEA counterpart ($3.95GJ/t_{CO2}$). Wang et al. (2019) proposed [Bmim][NTf_2] for CO_2/H_2S removal from syngas attaining CO_2 and H_2S recoveries of 97.6% and 95.3%. Aghaie et al. (2018) reviewed IL-based CO_2 capture processes focusing on process engineering and thermodynamics.

Recently, Barbosa et al. (2019) disclosed a new process for decarbonation of raw water-saturated CO_2-rich NG (≈45%mol CO_2) using physical-sorbent IL [Bmim][NTf_2] at $P = 60$ bar and $T = 35^oC$. Its breakthrough resides in its low capture-ratio ($13.5kg^{IL}/kg^{NG}$) entailing low IL circulation rate, and its capacity of attaining full NG conditioning in a single step: starting with raw CO_2-rich NG, [Bmim][NTf_2] captures not only CO_2, but also water and C_3^+; i.e., it simultaneously executes CO_2 removal, WDPA and HCDPA, with final products lean NG ($CO_2 = 3\%mol$, $CH_4 = 92\%mol$, $H_2O = 4$ppm-mol, $P = 60$ bar), liquefied petroleum gas or LPG ($P = 5$ bar) and tradeable CO_2-rich EOR-Fluid ($CO_2 = 79\%mol$, $CH_4 = 16\%mol$, $P = 250$ bar). The strong point of this process is its selective primary stripping at high-pressure and high-temperature ($P = 50$ bar, $T = 250^oC$) releasing ≈93% of captured CO_2 and ≈100% of captured CH_4, taking advantage of high thermal stability of [Bmim][NTf_2]. A secondary stripping ($P = 5$ bar, $T = 252^oC$) liberates C3+/water and ≈7% of captured CO_2. This is a very different separation strategy of common IL-based decarbonation that capture only CO_2 releasing it via low-pressure stripping (Liu et al., 2016; Zareiekordshouli et al., 2018).

IL screening was addressed for NG decarbonation considering CO_2 solubility (Aki et al., 2004), CO_2/CH_4 selectivity (Carvalho and Coutinho, 2011) and heat-ratio (Zhang et al., 2016). Liu et al. (2016) screened [Bmim][NTf_2] as the most suitable IL for shale-gas decarbonation using viscosity, toxicity and molecular-simulated Henry constants to predict CO_2 solubility and CO_2/CH_4 selectivity. Likewise, Zhao et al. (2017) screened ILs for CO_2/CH_4 separation from 10,000 ILs considering toxicity, bioaccumulation, viscosity, melting-point, absorption capacity and selectivity, while Mota-Martinez et al. (2017) developed an IL screening based on process performance.

1.1. The present work

Despite several literature studies on IL screening, few consider properties relevant to environmental and engineering features concurrently to CO_2 solubility and heat-ratio, the most focused aspects. This work presents an original multi-criterial IL screening for NG decarbonation based on cost, absorption-related properties (density, viscosity, heat capacity, boiling-point), CO_2 loading, heat-ratio, pressure/temperature absorption-regeneration differentials ($\Delta P^{Abs\text{-}Reg}$, $\Delta T^{Abs\text{-}Reg}$) and environmental impacts toxicity and biodegradability.

Similarly, previous assessments of IL-based decarbonation processes mainly considered economic performance. This work explores a new multi-criterial sustainability assessment of NG decarbonation processes, scoring processes via qualitative/quantitative metrics of environmental-economic-social aspects (Araújo et al., 2015). Metrics are aggregated into a single sustainability-degree vector ($\underline{SD}$) evoking a sustainability-based process ranking: the higher SD_k, the higher is process k sustainability. $\underline{SD}$ is used for sustainability assessment of new [Bmim][NTf_2]-based NG decarbonation process of Barbosa et al. (2019) against the conventional aqueous-MDEA NG decarbonation, proving that the former is much more cleaner and sustainable than the latter.

2. Methods

The procedure for the complete assessment of IL-based decarbonation of CO_2-rich NG has the following phases (Fig. 1).

Phase 1: New multi-criterial IL screening for decarbonation of CO_2-rich NG ranks ILs for decarbonation of CO_2-rich NG. The ranking is based on scoring IL properties, cost, CO_2 loading, heat-ratio, pressure/temperature absorption-regeneration differentials ($\Delta P^{Abs\text{-}Reg}$, $\Delta T^{Abs\text{-}Reg}$) and environmental impacts. Scores are aggregated into the performance-degree vector ($\underline{PD}$) for candidate ILs. The best IL has the highest performance-degree PD_k.

Phase 2: New IL-based cleaner decarbonation process for raw water-saturated CO_2-rich NG with IL [Bmim][NTf_2] prescribes selective CO_2/CH_4/water/C3+ stripping at high-pressure and high-temperature. This IL-based decarbonation was simulated in ASPEN-PLUS and compared to conventional aqueous-MDEA-based decarbonation of CO_2-rich NG. [Bmim][NTf_2] was confirmed as best IL from the new multi-criterial IL screening (Phase 1).

Phase 3: Multi-criterial sustainability assessment of decarbonation processes for CO_2-rich NG. The sustainability of IL-based and aqueous-MDEA-based decarbonation processes were assessed via qualitative/quantitative metrics aggregated into a sustainability-degree vector ($\underline{SD}$) of candidate processes; the higher SD_k, the higher process k sustainability.

2.1. Multi-criterial IL screening for decarbonation of CO_2-Rich NG

The important parameters for evaluating NG decarbonation solvents comprehend absorption capacity, absorption rate, regeneration heat-ratio, environmental impact, cost and operational

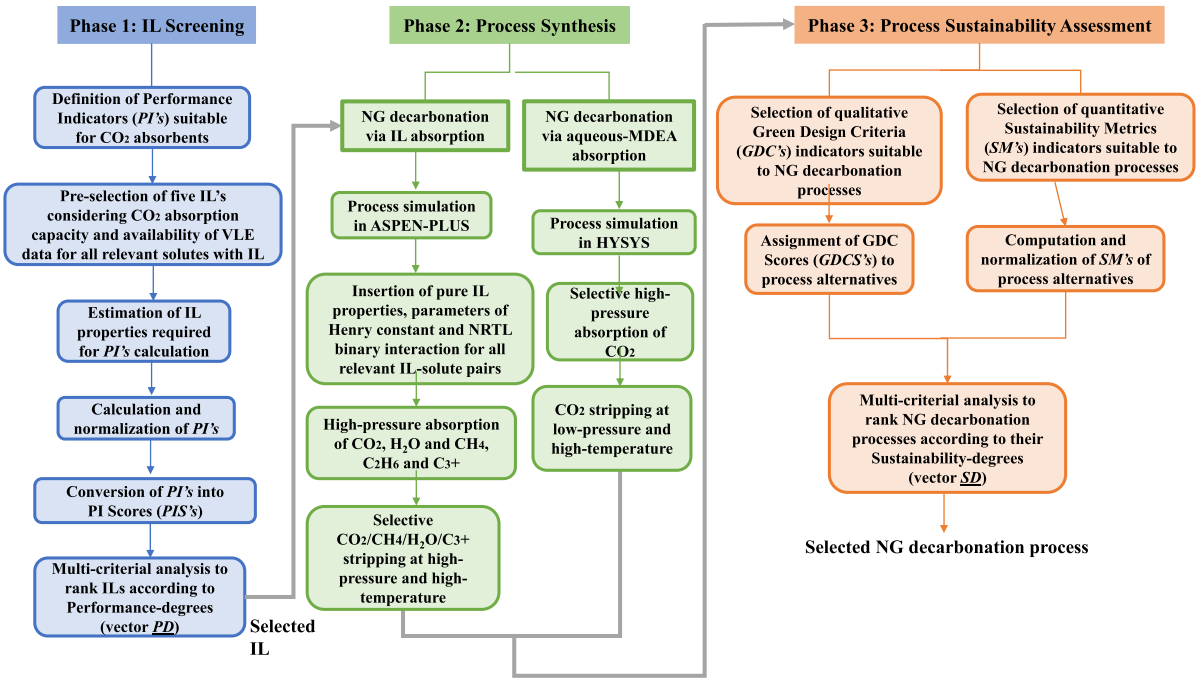

Fig. 1. Flowchart of IL screening, synthesis and sustainability analysis of IL-based NG decarbonation.

conditions (IEAGHG, 2014). Thus, the proposed multi-criterial IL screening focuses on scoring ILs according to performance-indicators (*PI's*) of environmental/technical aspects, toxicity and biodegradability.

From industrial perspective, IL properties (e.g., viscosity, density, heat capacity and boiling-point) must be known since they affect pumps, exchangers and column hydraulics. In general, ILs are denser (Singh and Kumar, 2008) and much more viscous than water (Branco et al., 2011). Additionally, solvent volatility and degradation impact replacement costs; in other words, solvents must be thermally and chemically stable with high boiling-points.

Lail et al. (2014) stated that to reduce costs of a solvent-based CO_2 capture the regeneration heat-ratio must be low. In conventional CO_2 capture, the reboiler heat-ratio (kJ/kgCO_2) consists of sensible heat to the regeneration temperature, CO_2 absorption heat and, for aqueous-solvents, water vaporization enthalpy. Thus, minimization of IL regeneration heat-ratio requires low IL heat capacity ($\overline{C}_p$) and absorption heat ($\Delta\overline{H}^{Abs}_{CO_2}$). Moreover, ILs can be regenerated by pressure-differential ($\Delta P^{Abs\text{-}Reg}$) and/or temperature-differential ($\Delta T^{Abs\text{-}Reg}$) between absorption and regeneration steps. Hence temperature/pressure conditions affecting driving forces for CO_2 absorption/desorption must be analyzed as well as the difference rich-loading minus lean-loading, the solvent working capacity (Boot-Handford et al., 2014).

Many ILs may enter into aquatic environments, entailing that toxicity and biodegradability must also be assessed. Previous studies showed that imidazolium-based ILs with short alkyl chain (C_4) present moderate toxicity, while those with $C_{12}/C_{16}/C_{18}$ chains are highly toxic. The same behavior occurs for phosphonium/ammonium/pyridinium based ILs. Ecotoxic texts are normally conducted with Daphnia magna due to its sensitivity to environment changes (Petkovic et al., 2011).

ILs can replace aqueous-amines if they have not only competitive thermodynamic/environmental characteristics, but also lower cost. Solvent cost is included in process investment and is obviously one of the technological hurdles of IL decarbonation (Budzianowski, 2016). Regardless high laboratory-scale IL costs and absence of large-scale price history, Plechkova and Seddon (2008) argue that high IL reutilization can lead to life-cycle costs equivalent to those of traditional solvents. Based on the exposed IL aspects, Fig. 2 shows the performance-indicators (*PI*) in the proposed IL screening.

2.1.1. Set of pre-selected candidates for multi-criterial IL screening

Since there is a huge number of cation-anion combinations, a reduced set of five emblematic ILs was pre-selected based on CO_2 absorption capacity and also considering the availability of vapor-liquid equilibrium (VLE) data at different pressures and temperatures, a requirement for adjusting VLE thermodynamic models. Zeng et al. (2017) stated that anions play a greater role on CO_2 solubility than cations. Aki et al. (2004) report CO_2 solubility on [Bmim] ILs increasing in the following anion order: $[NO_3] < [dca] < [BF_4] < [PF_6] < [TfO] < [NTf_2] <$ [methide]. Among these anions, $[BF_4]$, $[PF_6]$ and $[NTf_2]$ were pre-selected for constituting ILs with high CO_2 solubility and wide utilization in CO_2 capture (Anthony et al., 2005).

Although imidazolium ILs have received great attention, Carvalho et al. (2010) argued that phosphonium ILs can dissolve even larger CO_2 loadings with trihexyltetradecylphosphonium chloride ([Thtdp][Cl]) showing the highest performance. All these ILs are physical-sorbents; however, Carvalho et al. (2009) showed [Bmim][Ac] is chemical-sorbent exhibiting higher CO_2 solubility at low-pressures than other ILs.

Therefore, the following ILs were pre-selected for IL screening comprehending different important cations and anions, as well as, physical and chemical absorptions: (1) 1-butyl-3-methylimidazolium tetrafluoroborate ([Bmim][BF_4]); (2) 1-butyl-3-methylimidazolium hexafluorophosphate ([Bmim][PF_6]); (3) 1-butyl-3-methylimidazolium bis(trifluoromethylsulfonyl)imide ([Bmim][NTf_2]); (4) 1-butyl-3-methylimidazolium acetate ([Bmim][Ac]); and (5) trihexyltetradecylphosphonium chloride ([Thtdp][Cl]).

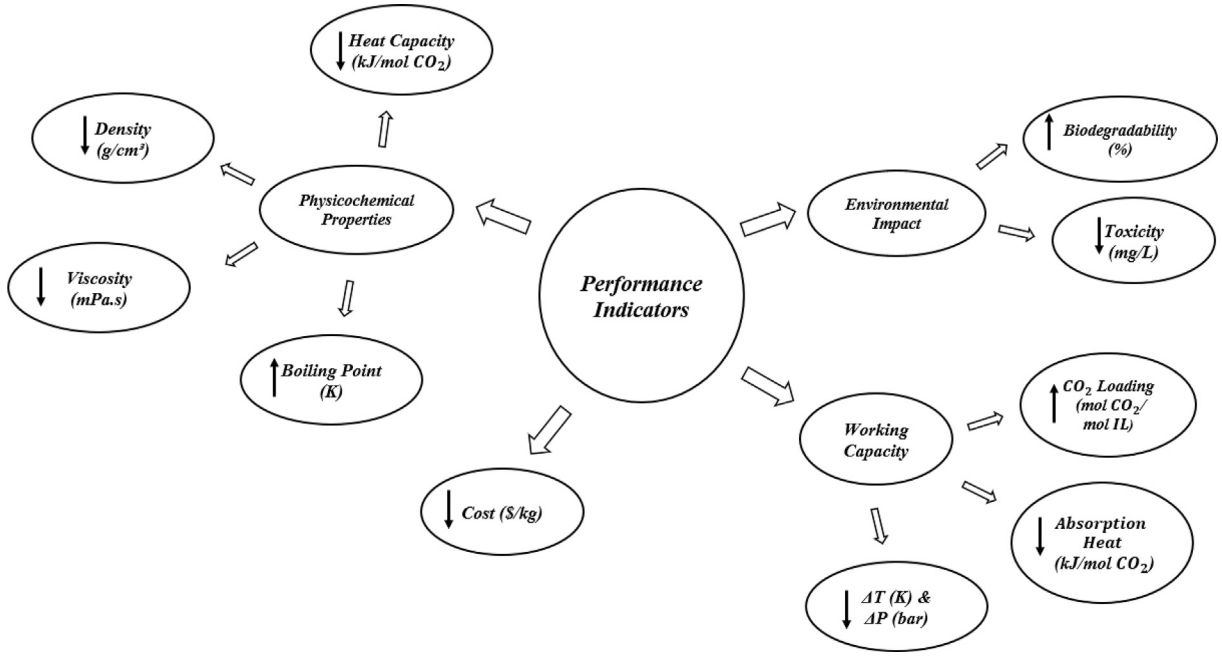

Fig. 2. Performance-indicators (*PI's*) for IL screening (arrows ≡ preferred trends).

2.1.2. Evaluation of IL performance-indicators

Values of biodegradability, toxicity and cost were taken from the literature. Pure IL properties (density, viscosity, heat-capacity and boiling-point), Henry constant parameters and NRTL binary interaction parameters – necessary for predicting CO_2 loading and absorption heat – were estimated via non-linear regressions over large sets of data of pure IL properties and binary IL-solute VLE for all solutes pertinent to the CO_2-rich NG context (CO_2/CH_4/H_2O/C_2H_6/C_3H_8/iC_4H_{10}/C_4H_{10}/iC_5H_{12}/C_5H_{12}/C_6H_{14}/C_7H_{16}/C_8H_{18}/C_9H_{20}/$C_{10}H_{22}$). Such regressions were conducted in MATLAB (Supplement S1, Supplementary Materials). Performance-indicators are aggregated into the performance-degree vector (*PD*, Sec. 2.3) enabling to select the most suitable IL for NG decarbonation.

2.2. Process synthesis: IL NG decarbonation and Aqueous-MDEA NG decarbonation

The new CO_2-rich NG decarbonation process for offshore rigs prescribing high-pressure absorption with [Bmim][NTf_2] (Barbosa et al., 2019) is compared to aqueous-MDEA NG decarbonation. Water-saturated CO_2-rich NG (≈45%mol CO_2) is the raw feed of processes. CO_2 removal at such conditions creates a technological IL niche due to high CO_2 fugacity in high-pressure raw NG favoring physical-absorption. The new IL-based decarbonation process captures not only CO_2, but also CH_4/C_2H_6/water/C3+ in the high-pressure absorption and executes selective CO_2/CH_4/C_2H_6/water/C3+ stripping at high-pressure and high-temperature, accomplishing simultaneously WDPA + HCDPA and CO_2 removal for NG specification. Despite that, the present analysis is limited to the CO_2 capture system, hence decarbonated NG and CO_2 streams from both processes are not processed any further. The IL-based process is implemented in ASPEN-PLUS, while the aqueous-MDEA-based variant is simulated in HYSYS. Since [Bmim][NTf2] is a new component in ASPEN-PLUS, its properties, as well as Henry constants parameters and NRTL binary interaction parameters for all IL-solute pairs of interest – IL-CO_2/IL-CH_4/IL-H_2O/IL-C_2H_6/IL-C_3H_8/IL-C_4H_{10}, IL-iC_4H_{10}/IL-iC_5H_{12}/IL-C_5H_{12}/IL-C_6H_{14}/IL-C_7H_{16}/IL-C_8H_{18}/IL-C_9H_{20}/IL-$C_{10}H_{22}$ – are necessary for VLE modeling and come from Barbosa et al. (2019). Table 1 shows the assumptions for simulation, while Figs. 3 and 4 show IL-based and aqueous-MDEA-based absorption processes for decarbonation of CO_2-rich NG. In both cases, raw CO_2-rich NG is fed at the absorber bottom ($P = 60$ bar, $T = 35°C$) counter-currently with IL. Lean NG leaves the column top, while rich IL leaves as bottoms and goes to regeneration. IL physical-sorbents are regenerated via depressurization and/or heating. In the new [Bmim][NTf2]-based decarbonation of CO_2-rich NG, rich IL expands a little to $P = 50$ bar and heats to $T = 250°C$ with hot lean IL and thermal-fluid (TF, $T = 280°C$). Since [Bmim][NTf2] is thermally stable, it resists to $T = 250°C$ (Meine et al., 2010). Unlike aqueous-MDEA, [Bmim][NTf2] also absorbs some CH_4, C_2H_6 and all C_3^+/H_2O. Thus, hot rich IL goes to adiabatic stripper#1 ($T = 250°C$, $P = 50$ bar) where CO_2, CH_4, C_2H_6 and some C_3^+/water are stripped at high-pressure. Stripper#1 vapor cools down to $T = 35°C$ with cooling-water (CW) recovering C_3^+/water. Stripper#1 IL expands to $P = 5$ bar and feeds adiabatic stripper#2 ($T = 252°C$, $P = 5$ bar) stripping low-pressure C_3^+. Stripper#2 vapor cools down to $T = 35°C$ with CW, recovering C_3^+ exported as liquefied petroleum gas (LPG). After C_3^+ removal, the residual CO_2-rich gas ($P = 5$ bar) is compressed to $P = 50$ bar and joins the CO_2-rich gas from stripper#1, forming the CO_2 Product (Fig. 3). The liquids from knock-out vessels ($P = 15$, $P = 50$ bar) are respectively expanded to $P = 5$ bar and $P = 1$ bar for C_3^+/water condensation. In IL-based process, all water from raw CO_2-rich NG is first captured by IL, then vaporized in stripper#1 and stripper#2, expanded to $P = 1$ bar after condensation for decarbonation, and finally leaves as an outlet (H_2O Out). Vapors from water stripping at $P = 1$ bar (Vent) are flared.

In the aqueous-MDEA process, solvent is regenerated via low-pressure stripping. Stripped CO_2 is compressed to $P = 50$ bar to meet the same pressure of CO_2 Product (Fig. 4) from IL-based process. The CO_2 streams from both processes have high water content ($T = 35°C$, $P = 50$ bar), but CO_2 dehydration is not considered. Only the water condensed in knock-out vessels is considered and recycled to the stripping column of aqueous-MDEA-based process.

Table 1
Simulation assumptions: IL-based and aqueous-MDEA-based processes.

Item	Description	Assumptions
{F1}	Simulation	Aqueous-MDEA Process: ASPEN-HYSYS; IL Process with [Bmim][NTf2]: ASPEN-PLUS.
{F2}	Thermodynamic Models	Gas, CO2 and Hydrocarbon Processing: Peng-Robinson EOS (PR-EOS); Aqueous-MDEA Operations: HYSYS Acid-Gas Package; [Bmim][NTf2] Operations: Liquid = NRTL; Gas = Redlich-Kwong EOS (RK-EOS) (Barbosa et al., 2019).
{F3}	Raw NG Feed (%mol composition)	5.48 MMsm3/d; P = 60 bar; T = 35°C; 43.93%CO2, 49.92%CH4, 3%C2H6, 2%C3H8, 0.3% i-C4H10, 0.2%C4H10, 0.2% i-C5H12, 0.1%C5H12, 0.1%C6H14, 0.05%C7H16, 0.03%C8H18, 0.01%C9H20, 0.01%C10H22, 1652.8 ppm-mol H2O.
{F4}	NG Product	CO2≤3%mol.
{F5}	CO_2 Product	P = 49.5 bar.
{F6}	Aqueous-MDEA Absorption	10-Staged; P = 60 bar; Lean-Solvent (%w/w): 49.95%MDEA, 49.95%H2O, 0.1%CO2; Capture-Ratio: 6.21 kgSolvent/kgNG;
{F7}	Aqueous-MDEA Stripping	10-Staged, P = 2 bar, TReboiler = 124.3°C, TCondenser = 40°C
{F8}	IL Absorption	10-Staged; P = 60 bar; Lean IL Capture-Ratio: 12.34 kgSolvent/kgNG.
{F9}	IL Stripping	Adiabatic Stripper#1: P = 50 bar, TInlet = 250oC; Adiabatic Stripper#2: P = 5 bar.
{F10}	Heat Exchangers	ΔPGas = 0.5 bar, ΔPLiquid = 0.1 bar; ΔTApproach = 5°C.
{F11}	Cold Utility	Cooling-Water (CW): TInlet/TOutlet = 30°C/45°C.
{F12}	Cold Heat-Sink	Seawater (SW): TInlet/TOutlet = 25°C/35°C.
{F13}	Compressor Stage	Adiab. Efficiency:75%; Driver: Electric; Compression-Ratio ≤ 3.5.
{F14}	Turbo-shafts	Heat-Power Ratio = 9705 KJ/KW.h.
{F15}	Intercoolers	Gas: TOutlet = 35°C; CW: TInlet = 30°C; ΔPGas = 0.5 bar.
{F16}	Waste-Heat Recovery Unit (WHRU)	PHW: P = 20 bar, TInlet/TOutlet = 100°C/190°C; THF: P = 4 bar, TInlet/TOutlet = 100°C/280°C;

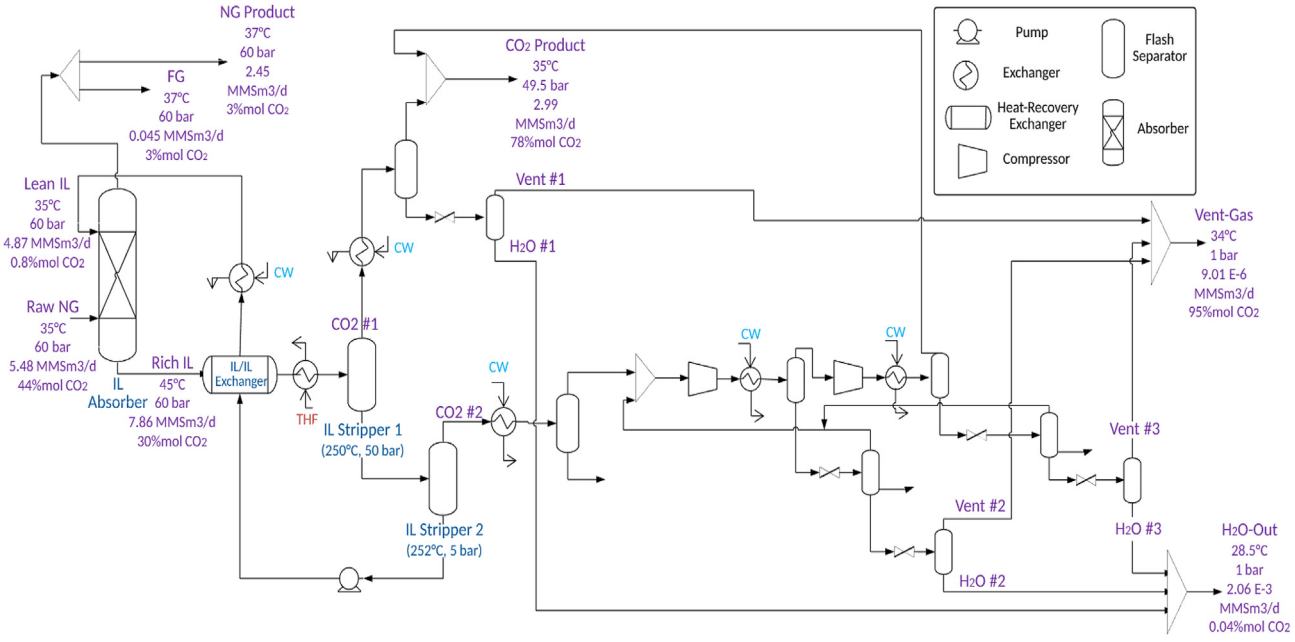

Fig. 3. IL absorption for decarbonation of CO_2-rich NG [FG: fuel-gas, CW: cooling-water, THF: thermal-fluid] (Barbosa et al., 2019).

2.3. Multi-criterial sustainability assessment: IL screening and process ranking

A modification of the multi-criterial sustainability analysis of Araújo et al. (2015) is proposed in the IL screening for NG decarbonation as well as to assess sustainability of NG decarbonation processes using [Bmim][NTf2] and aqueous-MDEA sorbents. For IL screening, the five ILs are scored based on performance-indicators (*PI's*) in Fig. 2, while for process sustainability analysis, the [Bmim][NTf2]-based and aqueous-MDEA-based processes are scored via qualitative green-design criteria (*GDC's*) metrics and quantitative sustainability metrics (*SM's*) for environmental-economic-social aspects. *PIs* are aggregated into a performance-degree vector (PD) and, similarly, *GDC's* and *SM's* are combined into the sustainability-degree vector (SD), which are calculated in next subsections. Fig. S2.1 (Supplement S2, Supplementary Materials) summarizes IL screening and sustainability analysis of decarbonation processes.

2.3.1. Performance-indicators: multi-criterial IL screening for NG decarbonation

Quantitative metrics corresponding to *PI's* (Table 2) are normalized according to Eqs. (1) and (2). Eq. (1) refers to *PI*'s that increase to increase IL performance (boiling-point, loading, biodegradation), whereas Eq. (2) refers to those behaving inversely

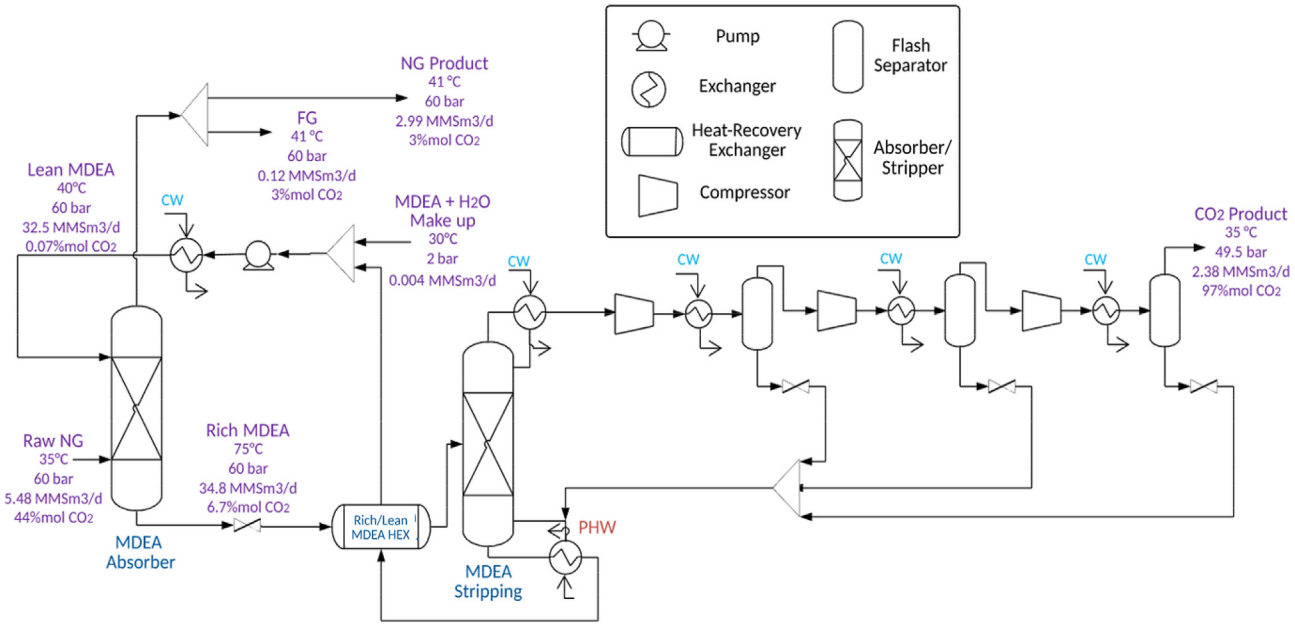

Fig. 4. Aqueous-MDEA absorption for decarbonation of CO_2-rich NG [FG: fuel-gas, CW: cooling-water, PHW: pressurized-hot-water].

Table 2
Performance-indicators: multi-criterial IL screening for NG decarbonation.

Performance- Indicator	Definition
PI#1	Density (gm/cm^3)@Lean-Loading
PI#2	Viscosity (mPa.s)@Lean-Loading
PI#3	Heat-Capacity (J/mol/K)@Lean-Loading
PI#4	Density (gm/cm^3)@Rich-Loading
PI#5	Viscosity (mPa.s)@Rich-Loading
PI#6	Heat-Capacity (J/mol/K)@Rich-Loading
PI#7	Boiling-Point (K)
PI#8	Absorption-Heat (kJ/mol)@Rich-Loading
PI#9	Maximum CO_2 Loading (molCO_2/mol IL)
PI#10	$\Delta P^{Abs\text{-}Reg}$ (bar) Absorption-Regeneration Pressure Difference
PI#11	$\Delta T^{Abs\text{-}Reg}$ (K) Absorption-Regeneration Temperature Difference
PI#12	Solvent-Cost (USD/kg) − Laboratory-Scale
PI#13	Toxicity EC50 (Daphnia Magna - 48h Immobilization Test) (mg/L)
PI#14	Biodegradation (sphingomonas paucimobilis bacterium - 28d) (%)

(density, viscosity, heat capacity, toxicity, absorption heat, $\Delta T^{Abs\text{-}Reg}$, $\Delta P^{Abs\text{-}Reg}$). $NPI_{i,j}$ represents the jth normalized performance-indicator ($j = 1, \cdots ni$) for the ith solvent ($j = 1, \cdots ns$). Scores are attributed to each element of (ns x ni) matrix NPI creating (ns x ni) matrix PIS as follows: (i) $PIS_{i,j} = 1$ (Good Performance), if $NPI_{i,j} = 0$; (ii) $PIS_{i,j} = 3$ (Average Performance), if $NPI_{i,j} \leq 0.5$; (iii) $PIS_{i,j} = 9$ (Poor Performance), if $NPI_{i,j} > 0.5$. Since choosing $\{1,3,9\}$ for scoring is arbitrary, the analysis is also done for $\{1,2,3\}$ to show that the same final IL ranking results.

$$NPI_{i,j} = \left(PI_j^{Greatest} - PI_{i,j}\right) \Big/ \left(PI_j^{greatest} - PI_j^{least}\right) \quad (1)$$

$$NPI_{i,j} = \left(PI_j - PI_{i,j}^{least}\right) \Big/ \left(PI_j^{greatest} - PI_j^{least}\right) \quad (2)$$

PI's are estimated from simulated VLE data or gathered from literature, and normalized in Eqs. (1) and (2) as dimensionless indicators from zero to one.

2.3.2. Green-design criteria: sustainability analysis of NG decarbonation processes

Processes are scored according to qualitative green-design criteria (*GDC's*) metrics and quantitative sustainability metrics (*SM's*) for evaluation of environmental-economic-social performance. *GDC's* are chosen from heuristics criteria in Table 3 comprehending principles of green chemistry (Anastas and Warner, 1998) and green engineering (Abraham and Nguyen, 2003) according to their suitability to the processes at hand (Anastas and Zimmerman, 2003). Processes are scored in terms of *GDC's* creating (np x nc) matrix GDCS as follows: $GDCS_{i,j}$ is *1*, *3* or *9* if process i ($i = 1 \ldots np$) has respectively good, average or poor compliance to *GDC* j ($j = 1 \ldots nc$). As in Sec. 2.3.1, calculations are also done attributing $\{1,2,3\}$ in place of $\{1,3,9\}$ to show that the final process ranking is invariant.

2.3.3. Sustainability metrics

Table 4 presents the quantitative sustainability metrics (*SM's*) for process assessment. These metrics were proposed by Araújo et al. (2015) and Jensen at al. (2003) based on performance-indicators for absorption processes and defined such that the

Table 3
Heuristic criteria for multi-criterial sustainability analysis of processes.

Green-Design Criteria	Definition
GDC#1	Prevention: Green processes designed to avoid waste rather than to treat it.
GDC#2	Separation-Design: Separation/purification designed to minimize energy consumption and materials usage, preferentially at ambient (T, P).
GDC#3	Design-for-Reuse: Green processes designed for commercial "afterlife."
GDC#4	Maximize Mass-Efficiency: Green processes designed for maximum mass-efficiency.
GDC#5	Maximize Energy-Efficiency: Green processes designed for maximum energy-efficiency.
GDC#6	Maximize Space-Efficiency: Green processes designed for minimum space-demand.
CDC#7	Integrate-Flows: Green processes designed integrating available energy and materials flows.
GDC#8	Less-Hazardous-Flows: All material/energy inputs/outputs are inherently as non-hazardous as possible.
GDC#9	Safer-Auxiliary-Materials: Auxiliary materials are inherently as non-hazardous as possible and avoided whenever possible.
GDC#10	Communities-Engagement: Green processes conception engages communities and stakeholders in the development of engineering solutions.

Table 4
Metrics: multi-criterial sustainability analysis of decarbonation processes.

Dimension	Metric	Definition
Environmental	Hydrocarbon-Losses[a] (HC Losses)	$HC\ Losses = 1 - \eta_{CH_4}$
	Solvent-Intensity (SI)	$SI = kgsolvent/kgCO_2$
	Energy-Intensity (EI)[b]	$EI = kW_e/kgCO_2$
	CO_2 Emissions[c]	$CO_2 Emissions = kgCO_2^{Eq}/kgCO_2^{Cap}$
Economic	Life-Cycle Cost (LCC)[d]	$LCC = \frac{FCI + t*COM}{Prod^{Rate}*t}$ (USD/tCO$_2$)
	Pressure-Differential	$\Delta P^{Abs-Reg} = P^{Absorption} - P^{Regeneration}$ (bar)
Social	Toxicity [e]	LD50(g/kg)
	Corrosivity	m/year
	Explosiveness	%v/v air

t: operation life-time (t = 15 years). Life-Cycle Cost Assessment is in Supplement S3, Supplementary Materials.
[a] $\eta_{CH_4} \equiv CH_4$ recovery.
[b] Heat duties are multiplied by 0.39 for equivalent electric powers (kWe) (Dimitriou et al., 2015).
[c] $kgCO_2^{Eq} \equiv kgCO_2$ equivalent from NG-fired power generation; $kgCO_2^{Cap} \equiv kgCO_2$ captured.
[d] FCI(USD): Fixed Capital Investment, COM(USD/y): Cost of Manufacturing, $Prod^{Rate}$(t/y): Production Rate,
[e] LD50: 50% animal-test lethal dose.

lower the value, the greener the process. The *SM's* are normalized in Eq. (3), creating the (*nm x np*) matrix $\underline{\underline{NSM}}$, where $NSM_{i,j}$ represents *i*th normalized sustainability metric ($i = 1 \ldots nm$) for *j*th process ($j = 1 \ldots np$) and $< SM_i >$ represents the average *i*th metric over *np* processes.

$$NSM_{ij} = SM_{ij} / < SM_i > \quad (3)$$

2.3.4. Performance-degree: multi-criterial IL screening for decarbonation

Performance-indicator criticality-index (*ns x 1*) vector ($\underline{PICI}$) is proposed in Eq. (4) from (*ns x ni*) matrix $\underline{\underline{PIS}}$ (Sec. 2.3.1) and weighting (*ni x 1*) vector ($\underline{W}$) to weight decision-making priorities.

$$\underline{PICI} = \underline{\underline{PIS}} * \underline{W} \quad (4)$$

For weighting of performance-indicators, again three levels of importance apply. It is considered that CO_2 loading, heat absorption, $\Delta T^{Abs\text{-}Reg}$, $\Delta P^{Abs\text{-}Reg}$ and cost (*PI#8* to *PI#12*, Table 2) greatly influences environment-economic impacts, being valuated as *4*. Pure IL properties (*PI#1* to *PI#7*) and toxicity (*PI#13*) are intermediary and valuated as *2*. The lowest value *1* is attributed to biodegradation (*PI#14*) since few studies report such data. The *j*th element of $\underline{W}$ is obtained in Eq. (5), where $value_j$ is the value *{4,2,1}* attributed to *j*th *PI*.

$$W_j = value_j \Big/ \sum_{k=1}^{ni} value_k \quad (5)$$

The (*ns x 1*) vector of criticality-factors for IL screening $\underline{CF}^{ILScr}$ is given in Eq. (6) by the Hadamard product between the sum of *NPI's* for each solvent and (*ns x 1*) vector $\underline{PICI}$, where $\underline{1}$ represents the (*ni x 1*) vector of 1's. Based on $\underline{CF}^{ILScr}$, $\underline{PD}$ is given in Eq. (7), where cf_{REF} is the criticality-factor of the reference solvent with the highest performance (lowest CF^{ILScr}). $\underline{PD}$ allows selecting the IL with the highest performance for NG decarbonation; i.e., with highest PD_k.

$$\underline{CF}^{ILScr} = \underline{PICI} \circ \left(\underline{\underline{NPI}} * \underline{1} \right) \quad (6)$$

$$\underline{PD} = 100 * cf_{REF} \circ \Big/ \underline{CF}^{ILScr} \quad (7)$$

2.3.5. Sustainability-degree of NG decarbonation processes

From the (*np x nc*) matrix $\underline{\underline{GDCS}}$ and (*nc x 1*) vector $\underline{W}^{GDC}$ for weighting *GDC's* in terms of decision-making priorities, green-design critically-index (*np x 1*) vector $\underline{GDCI}$ is obtained in Eq. (8). For uniform weighting, elements of $\underline{W}^{GDC}$ are chosen as *1/nc*, where *nc* is the number of heuristic criteria. $GDCI_k$ grades *k*th process criticality to the environment.

$$\underline{GDCI} = \underline{\underline{GDCS}} * \underline{W}^{GDC} \quad (8)$$

To establish a sustainability-indicator for decision-making among processes, heuristic criteria and sustainability metrics are combined into the (*np x 1*) vector of criticality-factors $\underline{CF}^{Sust}$ for sustainability assessment of processes, defined in Eq. (9) as the sum of *NSM's* intensified by GDCI, where $\underline{1}$ represents the (*nm x 1*) vector of 1's. The (*ns x 1*) vector of sustainability-degrees SD is defined in Eq. (10), where cf_{REF} is the criticality-factor of the reference process, chosen as aqueous-MDEA-based NG decarbonation.

$$\underline{CF}^{Sust} = \underline{GDCI} \circ \left(\underline{\underline{NSM}} * \underline{1} \right) \quad (9)$$

$$\underline{SD} = cf_{REF} \circ \Big/ \underline{CF}^{Sust} \quad (10)$$

To evaluate the contribution of metrics to the overall severity of processes, the (*np x nm*) severity-process matrix $\underline{\underline{SP}}$ is obtained from $\underline{\underline{NSM}}$ intensified by GDCI, where $\underline{1}$ represents the (*nm x 1*) vector of 1's in Eq. (11). Finally, the severity-contribution matrix ($\underline{\underline{SC}}$) is defined in Eq. (12), where $SP_{i,j}$ represents element *ij* of $\underline{\underline{SP}}$.

$$\underline{\underline{SP}} = \left(GDCI * 1^{T} \right) \circ \underline{\underline{NSM}} \quad (11)$$

$$\underline{\underline{SC}} = 100 \cdot \begin{bmatrix} \dfrac{SP_{1,1}}{\sum_{j=1}^{nm} SP_{1,j}} & \cdots & \dfrac{SP_{1,nm}}{\sum_{j=1}^{nm} SP_{1,j}} \\ \cdots & \cdots & \cdots \\ \dfrac{SP_{np,1}}{\sum_{j=1}^{nm} SP_{np,j}} & \cdots & \dfrac{SP_{np,nm}}{\sum_{j=1}^{nm} SP_{np,j}} \end{bmatrix} \quad (12)$$

3. Results

Results are initially presented for multi-criterial IL screening for NG decarbonation. Process simulation results follow for [Bmim][NTf2]-based and aqueous-MDEA-based decarbonation processes. Then, the results of multi-criterial sustainability assessment of such decarbonation processes are presented. Either in multi-criterial IL screening as well as in multi-criterial process sustainability assessment, calculations are conducted with two sets of non-proportional attributable scores *{1,3,9}* and *{1,2,3}* to show invariance of conclusions regarding such arbitrary choices (Secs. 2.3.1 and 2.3.2).

3.1. Results: multi-criterial IL screening for decarbonation of CO_2-Rich NG

Table 5 presents values of performance-indicators (*PI's*, Table 2) for the pre-selected ILs (Sec. 2.1.1). Values of toxicity (Pretti et al., 2009; Samorì et al., 2007 and Zhao et al., 2007), biodegradation (Abrusci et al., 2011) and cost (www.molbase.com) were gathered from literature. Supplement S1 (Supplementary Materials) present the estimated pure IL properties, CO_2 loadings, and absorption heats. Temperature-dependent properties were estimated at lean-loading and rich-loading, while the absorption heat was evaluated only at rich-loading (Table 2). Table 5 lacks biodegradation data of [thtdp][Cl], but since this IL is highly toxic, its biodegradation is considered inexistent. Similarly, since no data was found for [Bmim][Ac] toxicity on *Daphnia magna*, the highest toxicity was attributed based on its extreme hazardousness to water according to its Material Safety Data Sheet (MSDS).

Fig. 5a–b displays matrix $\underline{\underline{PIS}}$ with scores attributed to ILs according to *PI's*, respectively using sets of attributable score values *{1,3,9}* and *{1,2,3}*. [Bmim][BF_4], [Bmim][PF_6] and [Bmim][NTf_2] show the worst performances for *PI#1* (Density@Lean-Loading), *PI#4* (Density@Rich-Loading), *PI#9* (CO_2 Loading), *PI#10* ($\Delta P^{Abs\text{-}Reg}$) and *PI#11* ($\Delta T^{Abs\text{-}Reg}$). These ILs are CO_2 physical-sorbents entailing lower CO_2 solubility; i.e., low CO_2 loading and high $\Delta P^{Abs\text{-}Reg}$ and $\Delta T^{Abs\text{-}Reg}$. However, as physical-sorbents, they impose lower heat-ratios for CO_2 stripping; not surprisingly they present the highest performance for *PI#3* (Heat-Capacity@Lean-Loading), *PI#5* (Heat-Capacity@Rich-Loading), *PI#6* (Viscosity@Rich-Loading) and *PI#8* (Absorption-Heat@Rich-Loading). As [Bmim][Ac] is a CO_2 chemical-sorbent, it achieves the highest *PI#3* performance (Heat-Capacity@Lean-Loading) and *PI#9* (CO_2 Loading) and the worst *PI#8* performance (Absorption-Heat@Rich-Loading), a consequence of CO_2-IL chemical bonds. [Thtdp][Cl] is the only IL with a different cation, showing the lowest *PI#1* (Density@Lean-Loading), *PI#4* (Density@Rich-Loading), *PI#10* ($\Delta P^{Abs\text{-}Reg}$) and *PI#11* ($\Delta T^{Abs\text{-}Reg}$), as well as the highest *PI#7* (Boiling-Point).

With the normalized performance-indicators matrix ($\underline{\underline{NPI}}$) and the two matrices $\underline{\underline{PIS}}$ in Fig. 5a–b, vectors $\underline{PICI}$, $\underline{CF}^{ILScr}$ and $\underline{PD}$ are respectively calculated in Eqs. (13a) and (13b) for ILs [Bmim][BF_4], [Bmim][PF_6], [Bmim][NTf_2], [Bmim][Ac] and [Thtdp][Cl]).

Table 5
IL performance-indicators.

PI	Unit	[Bmim][BF_4]	[Bmim][PF_6]	[Bmim][NTf_2]	[Bmim][Ac]	[Thtdp][Cl]
PI#1	g/cm^3	1.1908	1.4335	1.3359	1.0402	0.872
PI#2	mPa.s	15.87	10.70	117.54	209.80	148.86
PI#3	J/mol.K	390.63	564.57	404.88	384.00	843.46
PI#4	g/cm^3	1.2322	1.4335	1.3758	1.0401	0.9026
PI#5	mPa.s	255.45	106.97	979.60	209.80	2752
PI#6	J/mol.K	360.40	514.74	389.77	383.98	787.35
PI#7	K	495.22	554.58	862.44	660.87	1006.15
PI#8	kJ/mol	14.4915	10.1181	5.7178	40.57	13.72
PI#9	mol CO_2/mol IL	0.5132	0.5511	0.7274	1.1677	0.3807
PI#10	bar	19	19	16.38	19	5.95
PI#11	K	65	65	33.6	50	0
PI#12	USD/kg	315	334	1687	971	1196
PI#13	mg/L	5.18	24	18.91	Extremely hazardous to water	0.072
PI#14	%	43	65	90	10	-

$$\underline{PICI} = \begin{bmatrix} 6.0811 \\ 5.5946 \\ 5.9730 \\ 5.7568 \\ 5.3243 \end{bmatrix}, \quad \underline{CF}^{ILScr} = \begin{bmatrix} 36.8921 \\ 30.4707 \\ 27.8257 \\ 35.4886 \\ 31.2468 \end{bmatrix}, \quad \underline{PD} = \begin{bmatrix} 75 \\ 91 \\ 100 \\ 78 \\ 89 \end{bmatrix} \tag{13.a}$$

$$\underline{PICI} = \begin{bmatrix} 2.4054 \\ 2.3243 \\ 2.4054 \\ 2.3514 \\ 2.1351 \end{bmatrix}, \quad \underline{CF}^{ILScr} = \begin{bmatrix} 14.5929 \\ 12.6593 \\ 11.2058 \\ 14.4953 \\ 12.5304 \end{bmatrix}, \quad \underline{PD} = \begin{bmatrix} 77 \\ 89 \\ 100 \\ 77 \\ 89 \end{bmatrix} \tag{13.b}$$

Either with attributable scores *{1,3,9}* or *{1,2,3}*, both performance-degrees vectors ($\underline{PD}$) in Eqs. (13.a) and (13.b) indicate in unison IL [Bmim][NTf_2] as the best decarbonation sorbent. [Bmim][NTf_2] has lower Heat-Capacity and Absorption-Heat and higher Boiling-Point than MDEA, despite its high $\Delta P^{Abs\text{-}Reg}$ (*PI#10*) and $\Delta T^{Abs\text{-}Reg}$ (*PI#11*). It is worth noting that the new [Bmim][NTf_2]-based decarbonation process for CO_2-rich NG of Barbosa et al. (2019) operates with much lower $\Delta P^{Abs\text{-}Reg} = 10$ bar (Sec. 2.2). $\underline{PD}$ was calculated using non-uniform weights ($\underline{W}$) attributed to *PI's* (Sec. 2.3.4). In case of uniform ($\underline{W}$) weighting, [Bmim][NTf_2] still has the highest $\underline{PD}$ component for both sets of attributable scores.

3.2. Performances of NG decarbonation processes

The new [Bmim][NTf_2]-based NG decarbonation (Barbosa et al., 2019) and the aqueous-MDEA counterpart were simulated using Table 1. Tables 6 and 7 present results of [Bmim][NTf_2]-based and aqueous-MDEA-based NG decarbonation processes. [Bmim][NTf_2]-based process has 63.7% lower power consumption thanks to high-pressure CO_2 stripping and, consequently, burns less fuel-gas (*0.*045 $MMsm^3/d$ *vs 0.*12$MMsm^3/d$). Despite the heat demand for IL stripping at $T = 250°C$, [Bmim][NTf_2]-based process demands 84% less heat. This results from the high water vaporization for CO_2 stripping in the aqueous-MDEA-based process, while the heat to strip solutes in [Bmim][NTf_2]-based process corresponds to sensible heat and vaporization enthalpies of light gases and traces of water (Lail et al., 2014). Furthermore, the CO_2 absorption enthalpy is higher for aqueous-MDEA relative to physical-sorbent [Bmim][NTf_2] (Chinn et al., 2005). This thermal advantage, however, is not taken further since heat is abundantly available in offshore rigs (see economic assumptions, Supplement S3, Supplementary Materials). The CO_2 product (EOR-Fluid) from [Bmim][NTf_2]-based process has lower CO_2 content (*78.1%mol vs 97.3%mol*), as aqueous-MDEA-based process has higher CO_2/CH_4 selectivity. On the other hand, [Bmim][NTf_2]-based process delivers a slightly higher flow rate of CO_2 product (178 t/h *vs* 176 t/h). Despite its flared vents, [Bmim][NTf_2]-based process has 64% less emissions thanks to its lower power consumption.

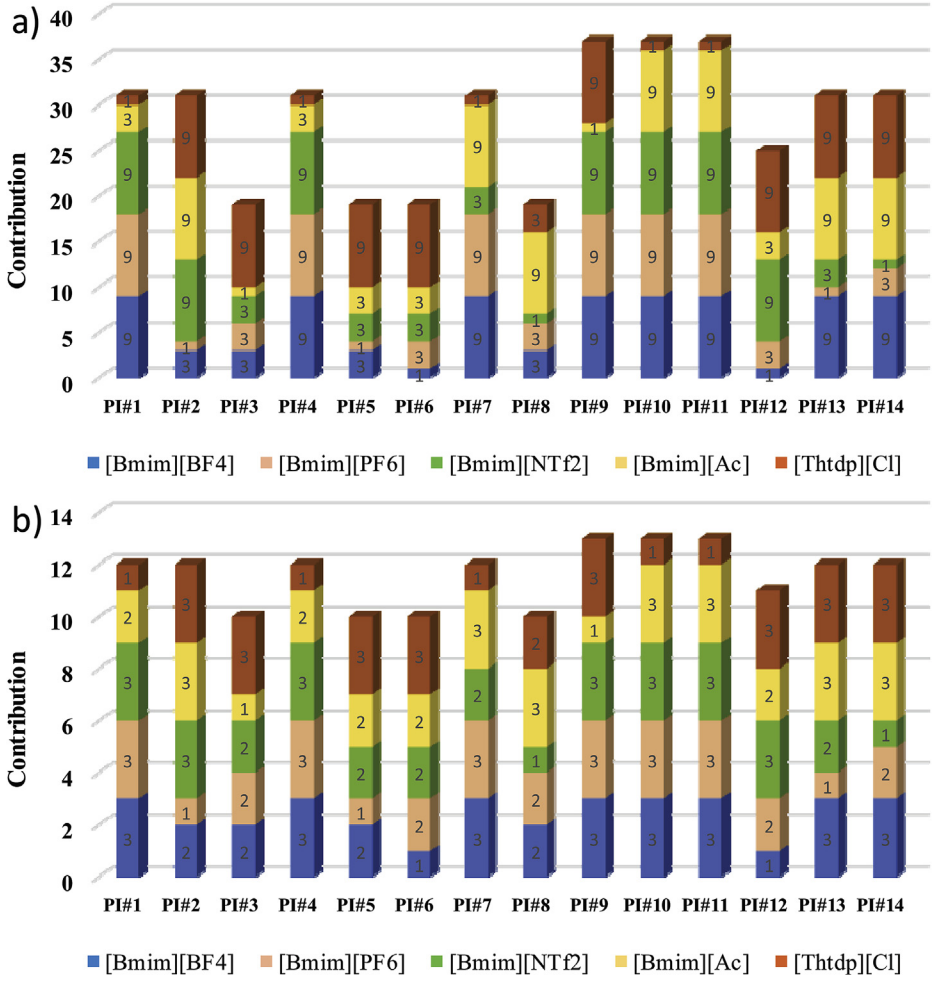

Fig. 5. Matrix $\underline{\underline{PIS}}$ with IL scores (a) *{1,3,9}* and (b) *{1,2,3}* according to performance-indicators (Table 5).

Table 6
Products: IL-based and aqueous-MDEA-based NG decarbonation processes.

	[Bmim][NTf_2] Process					Aqueous-MDEA Process		
	NG Product	Fuel-Gas (FG)	CO_2 Product	H_2O-Out	Vent-Gas	NG Product	Fuel-Gas (FG)	CO_2 Product
T (°C)	37	37	35	28.5	34	40.6	40.6	35
P (bar)	60	60	49.5	1	1	60	60	49.5
MMsm^3/d	2.45	0.045	2.99	2.06E-3	9.01E-6	2.99	0.12	2.38
***% CO_2**	3.00	3.00	78.13	0.04	94.79	3.03	3.03	97.29
% CH_4	91.73	91.73	15.06	0.00	0.00	86.96	86.96	1.43
% C_2H_6	4.21	4.21	1.99	0.00	0.00	5.18	5.18	0.14
% C_3H_8	1.01	1.01	2.82	0.00	0.00	3.46	3.46	0.08
% C_4H_{10}	0.01	0.01	0.36	0.00	0.00	0.35	0.35	0.01
% i-C_4H_{10}	0.03	0.03	0.53	0.00	0.00	0.52	0.52	0.01
%C_5H_{12}	0.00	0.00	0.18	0.00	0.00	0.08	0.08	0.13
% i-C_5H_{12}	0.01	0.01	0.36	0.00	0.00	0.20	0.20	0.21
% C_6H_{14}	0.00	0.00	0.18	0.00	0.00	0.01	0.01	0.22
% C_7H_{16}	0.00	0.00	0.09	0.00	0.00	0.00	0.00	0.11
% C_8H_{18}	0.00	0.00	0.05	0.00	0.00	0.00	0.00	0.07
% C_9H_{20}	0.00	0.00	0.01	0.00	0.00	0.00	0.00	0.02
% $C_{10}H_{22}$	0.00	0.00	0.01	0.00	0.00	0.00	0.00	0.02
% H_2O	-	-	0.23	99.96	5.21	0.21	0.21	0.27
ppm H_2O	3.5	3.5	-	-	-	-	-	-

*%mol compositions.

Table 7
CO_2 emissions, power, heat and fuel-gas consumptions.

Item	[Bmim][NTf_2] Process	Aqueous-MDEA Process
Power Consumption (MW)	6.6 (-63.7%*)	18.2
Heat Consumption (MW)	30.5 (-84.0%*)	191.2
Fuel-Gas Burnt (t/h)	1.4 (-63.1%*)	3.8
CO_2 Emissions (t/h)	3.7 (-64.0%*)	10.3
CO_2-Rich EOR-Fluid (t/h)	178(+ 1.1%*)	176

*Relative to aqueous-MDEA process.

A great difference between the new [Bmim][NTf_2]-based process (Barbosa et al., 2019) and the IL-based decarbonation of Zubeir et al. (2018) is the capability of the former to execute, simultaneously with decarbonation, water/C3+ removal, this way solving, in a single step, three major problems of raw NG conditioning: WDPA + HCDPA and decarbonation.

3.3. Sustainability analysis of NG decarbonation processes

The multi-criterial sustainability assessment (Sec. 2.3) of NG decarbonation processes is applied to [Bmim][NTf_2]-based absorption and aqueous-MDEA-based absorption. The scores assigned to each process according to *GDC's* (Table 3) are depicted in Fig. 6a and b, respectively using sets of attributable score values *{1,3,9}* and *{1,2,3}*.

Aqueous-MDEA-based process presents worst performance (highest scores) for all *GDC's* except *GDC#4*, *GDC#7* and *GDC#10*. Since *GDC#4* measures mass-efficiency, and CO_2/CH_4 selectivity is higher in aqueous-MDEA-based process, it complies better with *GDC#4*. *GDC#7* indicates compliance to the principle "*Integrate-Flows*", which is evaluated via $\Delta T^{Abs\text{-}Reg}$. Both processes thermally integrate lean-solvent and rich-solvent, but while $\Delta T^{Abs\text{-}Reg}$ is higher in [Bmim][NTf_2]-based process, aqueous-MDEA-based process complies better with *GDC#7*. Finally, aqueous-MDEA-based process is a mature technology, while IL-based processes are still in pilot stages (Almeida et al., 2017). Hence, there is higher community-engagement for aqueous-MDEA-based process entailing higher compliance with *GDC#10*.

Table 8 shows sustainability metrics with some values from literature (toxicity, corrosivity and explosiveness) and others from simulation results (Sec. 3.2) according to Table 4 (the lower the value, the cleaner the process). Hydrocarbon-Losses (*HC Losses*) and Solvent-Intensity (*SI*) indicate aqueous-MDEA-based process as the most suitable, while Energy-Intensity (*EI*) and CO_2 Emissions indicate [Bmim][NTf_2]-based process as the cleanest. The underlying reason is the physical-absorption nature of [Bmim][NTf_2]-based process, while aqueous-MDEA-based process executes chemical-absorption, entailing higher CO_2 solubility in aqueous-MDEA than in IL (lower *SI*) as well as a higher CO_2/CH_4 selectivity (lower *HC Losses*) and higher heat-ratio for solvent regeneration (higher *EI*). Besides the heat-ratio, *EI* and CO_2 Emissions are also influenced by power consumption, which is lower for [Bmim][NTf_2]-based process since it strips CO_2 at high-pressure, decreasing CO_2 compression power consumption.

Life-cycle cost (*LCC*) and $\Delta P^{Abs\text{-}Reg}$ indicate [Bmim][NTf_2]-based process as the most economically suitable. In fact, the new [Bmim][NTf_2]-based decarbonation process for CO_2-rich NG (Barbosa et al., 2019) has great economic performance (42.8% lower *LCC* relative to aqueous-MDEA process) influenced by CO_2 stripping at high-pressure (low $\Delta P^{Abs\text{-}Reg}$), which drastically decreases power consumption. Additionally, toxicity, corrosivity and explosiveness of ILs are lower than MDEA counterparts, indicating [Bmim][NTf_2] process as safer.

$\underline{GDCS}$ matrix, with *GDC* scores attributed to processes and $\underline{NSM}$ matrix, with normalized sustainability metrics, are combined as criticality-factors for sustainability assessment ($\underline{CF}^{Sust}$) and sustainability-degrees ($\underline{SD}$) in Eqs. (14a) and (14b), respectively using sets of attributable score values *{1,3,9}* and *{1,2,3}*. Components of $\underline{CF}^{Sust}$ and $\underline{SD}$ correspond, respectively, to [Bmim][NTf_2]-based and aqueous-MDEA-based processes. $\underline{SD}$ indicates that [Bmim][NTf_2]-based process is the most sustainable for decarbonation of CO_2-rich NG. This is expected since [Bmim][NTf_2]-based process presents lower heat and power consumptions, lower life-cycle cost and [Bmim][NTf_2] is a safer solvent. Either with attributable scores *{1,3,9}* or *{1,2,3}*, both sustainability-degrees vectors ($\underline{SD}$) in Eqs. (14.a) and (14.b) indicate [Bmim][NTf_2]-based NG decarbonation process as the more sustainable, but its sustainability-degree superiority reduces with *{1,2,3}*.

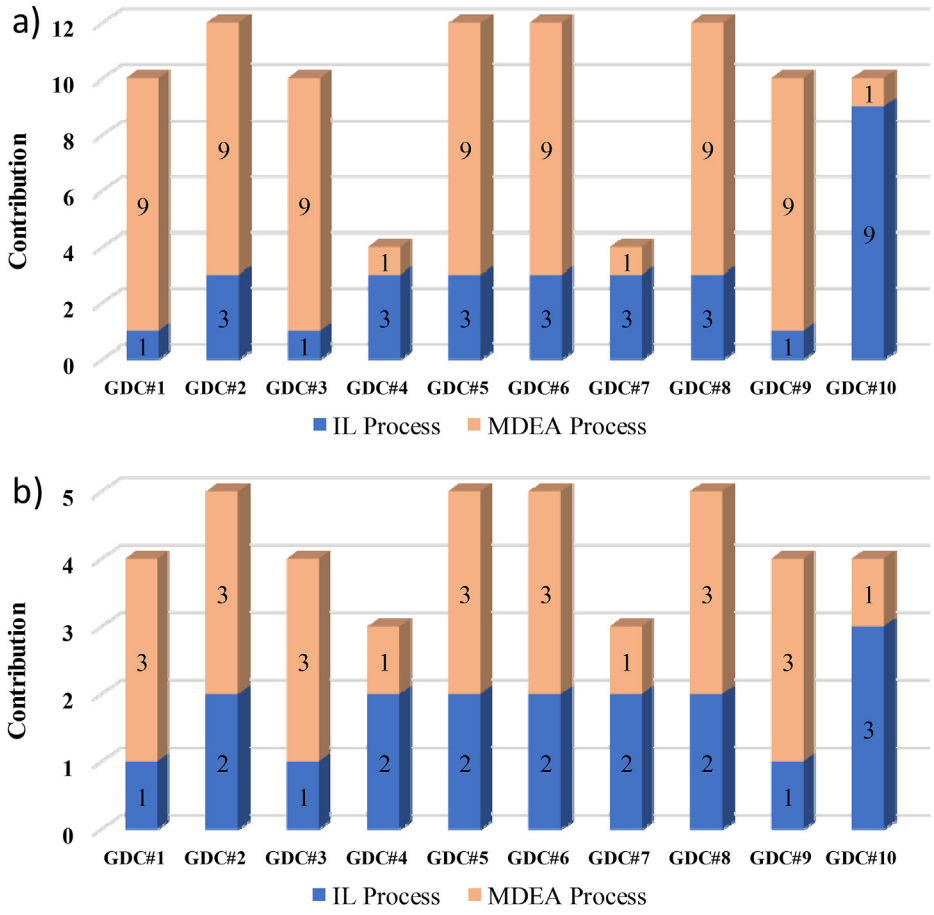

Fig. 6. Scores (a) *{1,3,9}* and (b) *{1,2,3}* of green-design criteria (*GDC's*) for IL-based and aqueous-MDEA-based NG decarbonation processes. (For interpretation of the references to colour in this figure legend, the reader is referred to the Web version of this article.)

Table 8
Computed sustainability metrics (*SM*, Table 4).

Dimension	Metric (unit)	IL Process	Aqueous-MDEA Process
Environmental	Hydrocarbon-Losses[a] (dimensionless)	0.164	0.012
	Solvent-Intensity[a] (kgSolvent/kgCO_2)	19.66	9.97
	Energy-Intensity[a] (kWe/kgCO_2)	0.10	0.53
	CO_2 Emissions[a] (kg CO_2/kgCO_2)	0.02	0.06
Economic	Life-Cycle Cost[a] (USD/tCO_2)	14.14	24.72
	Pressure Diferential[a] (bar)	10	58
Social	Toxicity[b] (g/kg)	54.5	300
	Corrosivity[b] (m/y)	1.10E-05	2.43
	Explosiveness[b] (%v/v air)	not explosive	0.9–8.4

[a]Metrics calculated from simulation results (Sec. 3.2).
[a]LCC is detailed in Supplement S3, Supplementary Materials.
[b]Metrics calculated from data in [Bmim][NTf2] MSDS (www.lookchem.com, 2017); MDEA Technical Bulletin (www.huntsman.com, 2017); Arenas and Reddy (2003); Eustaquio-Rincón et al. (2008); [Bmim][NTf_2] MSDS (www.merckperformancematerials.com, 2014) and MDEA MSDS (www.ilo.org, 2005).

$$\underline{CF}^{Sust} = \begin{bmatrix} 16.11 \\ 83.36 \end{bmatrix} \quad , \quad \underline{SD} = \begin{bmatrix} 5.17 \\ 1.00 \end{bmatrix} \tag{14.a}$$

$$\underline{CF}^{Sust} = \begin{bmatrix} 9.67 \\ 30.31 \end{bmatrix} \quad , \quad \underline{SD} = \begin{bmatrix} 3.14 \\ 1.00 \end{bmatrix} \tag{14.b}$$

Fig. 7 depicts the severity-contribution matrix ($\underline{SC}$) showing the contribution of each metric to the overall process-severity, which are invariant independently of the set of scores used (*{1,3,9}* or *{1.2.3}*). For IL-based process, the most important severity contributions are *HC Losses* and *SI*, while for aqueous-MDEA-based process these factors boost sustainability. All other metrics contribute to the overall severity of aqueous-MDEA-based process: corrosivity and explosiveness with highest contributions, followed by toxicity, $\Delta P^{Abs\text{-}Reg}$ and *EI*.

4. Conclusions

This work presents two main groups of results. Firstly, a new multi-criterial IL screening method was presented and used for selection of best IL for decarbonation of CO_2-rich NG. This new IL

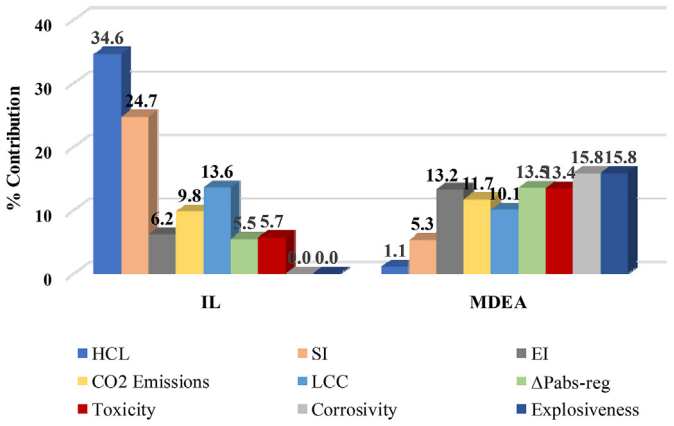

Fig. 7. Severity-contributions matrix $\underline{SC}$ and sustainability metrics *SM's* (Table 4) for IL-based and aqueous-MDEA-based decarbonation processes.

screening relies on performance-indicators calculated from IL literature data, IL environmental aspects, predicted pure IL properties, predicted VLE properties and CO_2 absorption performance.

Secondly, a process sustainability assessment, based on multi-criterial analysis with green-design criteria, was demonstrated for the aqueous-MDEA-based and the new [Bmim][NTf_2]-based NG decarbonation processes, the former using the best-ranked IL from the screening [Bmim][NTf2], which was pointed as the most suitable IL for NG decarbonation based on sustainability aspects.

[Bmim][NTf_2] was used in a totally new IL-based decarbonation of CO_2-rich NG via IL absorption. The main environmental and economic leverages of this new [Bmim][NTf_2]-based decarbonation lie on its selective CO_2/CH_4 stripping at high-pressure and high-temperature, which reduces power for dispatching CO_2 as EOR-Fluid.

The sustainability aspects of [Bmim][NTf_2]-based and aqueous-MDEA-based NG decarbonation processes were assessed for the same CO_2-rich raw NG feed. The sustainability-degree vector ($\underline{SD}$) indicates [Bmim][NTf_2]-based NG decarbonation as the most sustainable and cleaner alternative for decarbonation of CO_2-rich NG. The $\underline{SD}$ components corresponding to [Bmim][NTf_2]-based and to aqueous-MDEA-based processes attained *5.17* and *1* for attributable scores *{1,3,9}*. This superiority is also maintained for attributable scores *{1,2,3}*. In other words, the IL-based decarbonation of CO_2-rich NG is at least five times more sustainable (i.e., five times cleaner) than the aqueous-amine-based counterpart.

Other objects were calculated with $\underline{SD}$, like the severity-contribution matrix ($\underline{SC}$) and the severity-process matrix ($\underline{SP}$), the former allows identifying which metrics most influence process-severity, while the latter reports contribution of metrics to measure the overall process-severity. $\underline{SC}$ reveals (Fig. 7) that aqueous-MDEA-based NG decarbonation is less sustainable than the IL-based counterpart according to all sustainability metrics excepting *HC Losses* and *SI* due to the higher CO_2/CH_4 selectivity of aqueous-MDEA-based NG decarbonation thanks to its chemical-absorption nature.

It is worth noting that there are many studies on new ILs for CO_2 capture that were not considered here; most of them due to insufficient published data for model calibration in the IL screening. However, admitting that a better IL than [Bmim][NTf_2] for NG decarbonation could be found acting as a physical-sorbent, it merely would improve the IL-based process performance, without invalidating the conclusion that the IL-based NG decarbonation is cleaner and more sustainable than the conventional aqueous-MDEA-based counterpart. On the other hand, any IL chemical-sorbent would not be competitive against the [Bmim][NTf_2]-based NG decarbonation, because – as in the aqueous-MDEA-based process – its power consumption and emissions would be higher due to the necessary low-pressure CO_2 stripping.

Lastly, in a future work the same complete analysis including IL screening and sustainability assessment would be applied for flue-gas decarbonation. In this case, flue-gases have low CO_2 partial-pressure highly disfavoring physical-sorbents. Hence, a different IL – e.g., a chemical-sorbent IL – would be selected giving rise to a completely different process in the process synthesis phase (Fig. 1).

Acknowledgments

Authors acknowledge financial support from Petrobras SA (grant 2015/00383-2) and CNPq-Brazil (grant 311076/2017-3).

Appendix A. Supplementary data

Supplementary data to this article can be found online at https://doi.org/10.1016/j.jclepro.2019.118421.

Nomenclature

$Prod^{Rate}$	Production rate(t/y)
$\underline{CF}^{ILscr}$, $\underline{CF}^{sust}$	IL screening and process sustainability criticality-factors
Cf_{REF}	Reference criticality-factor
COM	Cost of manufacturing (*MMUSD/y*)
EI	Energy-intensity
FCI	Fixed capital investment (*MMUSD*)
GDC,$\underline{GDCI}$	Green-design criteria and green-design critically-index vector
$\underline{GDCS}$	Green-design criteria scores matrix
HC Losses	Hydrocarbon losses
LCC	Life-cycle cost *(USD/tCO$_2$)*
$\underline{NSM}$	Normalized sustainability-metrics matrix
$\underline{NPI}$	Normalized performance-indicators matrix
$\underline{PD}$, *PI*	Performance-degree vector, performance-indicator
$\underline{PICI}$	Performance-indicator criticality-index vector
$\underline{PIS}$	Performance-indicator scores matrix
$\underline{SC}$, $\underline{SP}$	Severity-contribution and severity-process matrices
$\underline{SD}$	Sustainability-degree vector
SI, SM	Solvent-intensity, sustainability metrics
$\underline{W}$, $\underline{W}^{GDC}$, $\Delta P^{Abs\text{-}Reg}$, $\Delta T^{Abs\text{-}Reg}$	Weighting vectors and Pressure/temperature absorption-regeneration differentials (bar,^{o}C)

References

Abraham, M.A., Nguyen, N., 2003. "Green engineering: defining the principles" - results from the san destin conference. Environ. Prog. 22 (4), 233–236. https://doi.org/10.1002/ep.670220410.

Abrusci, C., Palomar, J., Pablos, J.L., Rodriguez, F., Catalina, F., 2011. Efficient biodegradation of common ionic liquids by Sphingomonas paucimobilis bacterium. Green Chem. 13, 709–717. https://doi.org/10.1039/C0GC00766H.

Aghaie, M., Rezaei, N., Zendehboudi, S., 2018. A systematic review on CO2 capture with ionic liquids: current status and future prospects. Renew. Sustain. Energy Rev. 96, 502–525. https://doi.org/10.1016/j.rser.2018.07.004.

Aki, S.N., Mellein, B.R., Saurer, E.M., Brennecke, J.F., 2004. High-pressure phase behavior of carbon dioxide with imidazolium-based ionic liquids. J. Phys. Chem. B 108 (52), 20355–20365, 10. https://doi.org/10.1021/jp046895+.

Almeida, P.C., Araújo, O.Q.F., Medeiros, J.L., 2017. Managing offshore drill cuttings waste for improved sustainability. J. Clean. Prod. 165, 143–156. https://doi.org/10.1016/j.jclepro.2017.07.062.

Anastas, P.T., Warner, J.C., 1998. Green Chemistry: Theory and Practice. Oxford University Press, New York, 0198502346/9780198502340.

Anastas, P.T., Zimmerman, J.B., 2003. Design through the twelve principles of green

engineering. Environ. Sci. Technol. 37 (5), 94–101. https://doi.org/10.1021/es032373g.
Anthony, J.L., Anderson, J.L., Maginn, E.J., Brennecke, J.F., 2005. Anion effects on gas solubility in ionic liquids. J. Phys. Chem. B 109 (13), 6366–6374. https://doi.org/10.1021/jp046404l.
Araújo, O.Q.F., de Medeiros, J.L., Yokoyama, L., Morgado, C.R.V., 2015. Metrics for sustainability analysis of post-combustion abatement of CO2 emissions: microalgae mediated routes and CCS (carbon capture and storage). Energy 92, 556–568. https://doi.org/10.1016/j.energy.2015.03.116.
Arenas, M.F., Reddy, R.G., 2003. Corrosion of steel in ionic liquids. J. Min. Metall. Sect. B Metall. 39 (1–2), 81–91. http://www.jmmab.com/images/pdf/2003/csil-jul-2003-81-91.pdf.
Arinelli, L. de O., Trotta, T.A.F., Teixeira, A.M., de Medeiros, J.L., Araújo, O.Q.F., 2017. Offshore processing of CO2 rich natural gas with supersonic separator versus conventional routes. J. Nat. Gas Sci. Eng. 46, 199–221. https://doi.org/10.1016/j.jngse.2017.07.010.
Barbosa, L.C., Araújo, O.Q.F., de Medeiros, J.L., 2019. Carbon capture and adjustment of water and hydrocarbon dew-points via absorption with ionic liquid [Bmim][Ntf2] in offshore processing of CO2-rich natural gas. J. Nat. Gas Sci. Eng. 66, 26–41. https://doi.org/10.1016/j.jngse.2019.03.014.
Bermejo, M.D., Montero, M., Saez, E., Florusse, L.J., Kotlewska, A.J., Cocero, M.J., van Rantwijk, F., Peters, C.J., 2008. Liquid vapor equilibrium of the systems butylmethylimidazolium nitrate-CO2 and hydroxypropylmethylimidazolium nitrate-CO2 at high pressure: influence of water on the phase behavior. J. Phys. Chem. B 112, 13532–13541. https://doi.org/10.1021/jp802540j.
Boot-Handford, M.E., Abanades, J.C., Anthony, E.J., Blunt, M.J., Brandani, S., Mac Dowell, N., Fernández, J.R., Ferrari, M., Gross, R., Hallett, J.P., Haszeldine, R.S., Heptonstall, P., Lyngfelt, A., Makuch, Z., Mangano, E., Porter, R.T.J., Pourkashanian, M., Rochelle, G.T., Shah, N., Yao, J.G., Fennel, P.S., 2014. Carbon capture and storage update. Energy Environ. Sci. 130–189. https://doi.org/10.1039/C3EE42350F.
Branco, L.C., Carrera, G.V., Aires-de-Sousa, J., Martin, I.L., Frade, R., Afonso, C.A., 2011. Physico-Chemical Properties of Task-specific Ionic Liquids, Ionic Liquids: Theory, Properties, New Approaches. InTech. https://doi.org/10.5772/15560.
Budzianowski, W.M., 2016. Explorative analysis of advanced solvent processes for energy efficient carbon dioxide capture by gas–liquid absorption. Int. J. Greenh. Gas Control 49, 108–120. https://doi.org/10.1016/j.ijggc.2016.02.028.
Carvalho, P.J., Coutinho, J.A.P., 2011. The polarity effect upon the methane solubility in ionic liquids: a contribution for the design of ionic liquids for enhanced CO2/CH4 and H2S/CH4 selectivities. Energy Environ. Sci. 4, 4614–4619. https://doi.org/10.1039/C1EE01599K.
Carvalho, P.J., Alvarez, V.H., Marrucho, I.M., Aznar, M., Coutinho, J.A., 2010. High carbon dioxide solubilities in trihexyltetradecylphosphonium-based ionic liquids. J. Supercrit. Fluids 52 (3), 258–265. https://doi.org/10.1016/j.supflu.2010.02.002.
Carvalho, P.J., Álvarez, V.H., Schröder, B., Gil, A.M., Marrucho, I.M., Aznar, M., Santos, L.M.N.B.F., Coutinho, J.A.P., 2009. Specific solvation interactions of CO2 on acetate and trifluoroacetate imidazolium based ionic liquids at high pressures. J. Phys. Chem. B 113 (19), 6803–6812. https://doi.org/10.1021/jp901275b.
Chinn, D., Vu, D., Driver, M., Boudreau, L., CO2 removal from gas using ionic liquid absorbents, U.S. Patent 10/737090, 16 Jun. 2005.
de Medeiros, J.L., Barbosa, L.C., Araújo, O.Q.F., 2013. Equilibrium approach for CO2 and H2S absorption with aqueous solutions of alkanolamines: theory and parameter estimation. Ind. Eng. Chem. Res. 52, 9203–9226. https://doi.org/10.1021/ie302558b.
Dimitriou, I., García-Gutiérrez, P., Elder, R.H., Cuéllar-Franca, R.M., Azapagic, A., Allen, R.W., 2015. Carbon dioxide utilization for production of transport fuels: process and economic analysis. Energy Environ. Sci. 8 (6), 1775–1789. https://doi.org/10.1039/C4EE04117H.
Eustaquio-Rincón, R., Rebolledo-Libreros, M.E., Trejo, A., Molnar, R., 2008. Corrosion in aqueous solution of two alkanolamines with CO2 and H2S: N-methyldiethanolamine + diethanolamine at 393 K. Ind. Eng. Chem. Res. 47 (14), 4726–4735 [s.l.]. https://doi.org/10.1021/ie071557r.
Holmes, A.S., Ryan, J.M., 1982. Cryogenic Distillation Separation of Acid Gases from Methane. US patent US4318723 A.
Huang, Y., Zhang, X., Zhang, X., Dong, H., Zhang, S., 2014. Thermodynamic modeling and assessment of ionic liquid-based CO2 capture processes. Ind. Eng. Chem. Res. 53 (29), 11805–11817. https://doi.org/10.1021/ie501538e.
IEAGHG, 2014. Assessment of Emerging CO2 Capture Technologies and Their Potential to Reduce Costs, Report 2014/TR4. Accessed. https://ieaghg.org/docs/General_Docs/Reports/2014-TR4.pdf. (Accessed 15 September 2018).
Jensen, N., Coll, N., Gani, R., 2003. An integrated computer-aided system for generation and evaluation of sustainable process alternatives. Clean Technol. Environ. Policy 5, 209–235. https://doi.org/10.1007/s10098-003-0224-9.
Lail, M., Tanthana, J., Coleman, L., 2014. Non-aqueous solvent (NAS) CO2 capture process. Energy Procedia 63, 580–594. https://doi.org/10.1016/j.egypro.2014.11.063.
Leung, Y.C., Caramanna, G., Maroto-Valer, M.M., 2014. An overview of current status of carbon dioxide capture and storage technologies. Renew. Sustain. Energy Rev. 39, 426–443. https://doi.org/10.1016/j.rser.2014.07.093.
Liu, X., Huang, Y., Zhao, Y., Gani, R., Zhang, X., Zhang, S., 2016. Ionic liquid design and process simulation for decarbonisation of shale gas. Ind. Eng. Chem. Res. 55 (20), 5931–5944. https://doi.org/10.1021/acs.iecr.6b00029.
Ma, Y., Gao, J., Wang, Y., Hu, J., Cui, P., 2018. Ionic liquid-based CO2 capture in power plants for low carbon emissions. Int. J. Greenh. Gas Control 75, 134–139. https://doi.org/10.1016/j.ijggc.2018.05.025.
Meine, N., Benedito, F., Rinaldi, R., 2010. Thermal stability of ionic liquids assessed by potentiometric titration. Green Chem. 12 (10), 1711–1714. https://doi.org/10.1039/C0GC00091D.
Mota-Martinez, M.T., Hallett, J.P., Mac Dowell, N., 2017. Solvent selection and design for CO2 capture–how we might have been missing the point. Sustain. Energy Fuel. 1 (10), 2078–2090. https://doi.org/10.1039/C7SE00404D.
Petkovic, M., Seddon, K.R., Rebelo, L.P.N., Pereira, C.S., 2011. Ionic liquids: a pathway to environmental acceptability. Chem. Soc. Rev. 40, 1383–1403. https://doi.org/10.1039/C004968A.
Plechkova, N.V., Seddon, K.R., 2008. Applications of ionic liquids in the chemical industry. Chem. Soc. Rev. 37, 123–150. https://doi.org/10.1039/B006677J.
Pretti, C., Chiappe, C., Baldetti, I., Brunini, S., Monni, G., Intorre, L., 2009. Acute toxicity of ionic liquids for three freshwater organisms: pseudokirchneriella subcapitata, Daphnia magna and Danio rerio. Ecotoxicol. Environ. Saf. 72 (4), 1170–1176. https://doi.org/10.1016/j.ecoenv.2008.09.010.
Ramdin, M., de Loos, T.W., Vlugt, T.J.H., 2012. State-of-the-art of CO2 capture with ionic liquids. Ind. Eng. Chem. Res. 51 (24), 8149–8177. https://doi.org/10.1021/ie3003705.
Samorì, C., Pasteris, A., Galletti, P., Tagliavini, E., 2007. Acute toxicity of oxygenated and nonoxygenated imidazolium-based ionic liquids to Daphnia magna and Vibrio fischeri. Environ. Toxicol. Chem. 26 (11), 2379–2382. https://doi.org/10.1897/07-066R2.1.
Shiflett, M.B., Drew, D.W., Cantini, R.A., Yokozeki, A., 2010. Carbon dioxide capture using ionic liquid 1-Butyl-3-methylimidazolium acetate. Energy Fuel. 24 (10), 5781–5789. https://doi.org/10.1021/ef100868a.
Singh, G., Kumar, A., 2008. Ionic liquids: physico-chemical, solvent properties and their applications in chemical processes. Indian J. Chem. 47, 495–503. http://nopr.niscair.res.in/handle/123456789/2077.
Valencia-Marquez, D., Flores-Tlacuahuac, A., Vasquez-Medrano, R., 2017. An optimization approach for CO2 capture using ionic liquids. J. Clean. Prod. 168, 1652–1667. https://doi.org/10.1016/j.jclepro.2016.11.064.
Vega, L.F., Vilaseca, O., Lovell, F., Andreu, J.S., 2010. Modeling ionic liquids and the solubility of gases in them: recent advances and perspectives. Fluid Phase Equilib. 294, 1–2, 15–30. https://doi.org/10.1016/j.fluid.2010.02.006.
Wang, Y., Liu, X., Kraslawski, A., Gao, J., Cui, P., 2019. A novel process design for CO2 capture and H2S removal from the syngas using ionic liquid. J. Clean. Prod. 213, 480–490. https://doi.org/10.1016/j.jclepro.2018.12.180.
Zareiekordshouli, F., Lashanizadehgan, A., Darvishi, P., 2018. Study on the use of an imidazolium-based acetate ionic liquid for CO2 capture from flue gas in absorber/stripper packed columns: experimental and modeling. Int. J. Greenh. Gas Control 70, 178–192. https://doi.org/10.1016/j.ijggc.2018.02.002.
Zeng, S., Zhang, X., Bai, L., Zhang, X., Wang, H., Wang, J., Bao, D., Li, M., Liu, X., Zhang, S., 2017. Ionic-liquid-based CO2 capture systems: structure, interaction and process. Chem. Rev. 117 (14), 9625–9673. https://doi.org/10.1021/acs.chemrev.7b00072.
Zhang, Y., Ji, X., Xie, Y., Lu, X., 2016. Screening of conventional ionic liquids for carbon dioxide capture and separation. Appl. Energy 162, 1160–1170. https://doi.org/10.1016/j.apenergy.2015.03.071.
Zhao, D., Liao, Y., Zhang, Z.D., 2007. Toxicity of ionic liquids. Clean. - Soil, Air, Water 35 (n.1), 42–48. https://doi.org/10.1002/clen.200600015.
Zhao, Y., Gani, R., Afzal, R.M., Zhang, X., Zhang, S., 2017. Ionic liquids for absorption and separation of gases: an extensive database and a systematic screening method. AIChE J. 63 (4), 1353–1367. https://doi.org/10.1002/aic.15618.
Zubeir, L.F., Lacroix, M.H.M., Meuldijk, J., Kroon, M.C., Kiss, A.A., 2018. Novel pressure and temperature swing processes for CO2 capture using low viscosity ionic liquids. Separ. Purif. Technol. 204, 314–327. https://doi.org/10.1016/j.seppur.2018.04.085.